Energy level alignment at the methylammonium lead iodide/copper phthalocyanine interface

Chen, Shi; Goh, Teck Wee; Sabba, Dharani; Chua, Julianto; Mathews, Nripan; Huan, Cheng Hon Alfred; Sum, Tze Chien

2014

Chen, S., Goh, T. W., Sabba, D., Chua, J., Mathews, N., Huan, C. H. A., et al. (2014). Energy level alignment at the methylammonium lead iodide/copper phthalocyanine interface. APL materials, 2(8), 081512-.

https://hdl.handle.net/10356/105899

https://doi.org/10.1063/1.4889844

Energy level alignment at the methylammonium lead iodide/copper phthalocyanine interface

Shi Chen, Teck Wee Goh, Dharani Sabba, Julianto Chua, Nripan Mathews, Cheng Hon Alfred Huan, and Tze Chien Sum

Citation: APL Materials **2**, 081512 (2014); doi: 10.1063/1.4889844
View online: http://dx.doi.org/10.1063/1.4889844
View Table of Contents: http://scitation.aip.org/content/aip/journal/aplmater/2/8?ver=pdfcov
Published by the AIP Publishing

APL MATERIALS **2**, 081512 (2014)

Energy level alignment at the methylammonium lead iodide/copper phthalocyanine interface

Shi Chen,[1] Teck Wee Goh,[1] Dharani Sabba,[2,3] Julianto Chua,[2,3] Nripan Mathews,[2,3] Cheng Hon Alfred Huan,[1,4,a] and Tze Chien Sum[1,a]
[1]*Division of Physics and Applied Physics, School of Physical and Mathematical Sciences, Nanyang Technological University, 21 Nanyang Link, Singapore 637371, Singapore*
[2]*Energy Research Institute @NTU (ERI@N), Research Techno Plaza, X-Frontier Block, Level 5, 50 Nanyang Drive, Singapore 637553, Singapore*
[3]*School of Materials Science and Engineering, Nanyang Technological University, Nanyang Avenue, Singapore 639798, Singapore*
[4]*Institute of High Performance Computing, 1 Fusionopolis Way, #16–16 Connexis, Singapore 138632, Singapore*

(Received 17 May 2014; accepted 30 June 2014; published online 5 August 2014)

The energy level alignment at the $CH_3NH_3PbI_3$/copper phthalocyanine (CuPc) interface is investigated by X-ray photoelectron spectroscopy (XPS) and ultraviolet photoelectron spectroscopy (UPS). XPS reveal a 0.3 eV downward band bending in the CuPc film. UPS validate this finding and further reveal negligible interfacial dipole formation – verifying the viability of vacuum level alignment. The highest occupied molecular orbital of CuPc is found to be closer to the Fermi level than the valance band maximum of $CH_3NH_3PbI_3$, facilitating hole transfer from $CH_3NH_3PbI_3$ to CuPc. However, subsequent hole extraction from CuPc may be impeded by the downward band bending in the CuPc layer. [http://dx.doi.org/10.1063/1.4889844]

Methylammonium lead halide ($CH_3NH_3PbX_3$, X = I, Br, and Cl), which is also termed perovskite in short based on its crystal structure, have recently attracted extensive attention among the solar cell communities. Most recently, these perovskite solar cells have demonstrated record power conversion efficiencies (PCEs) of 19.3%,[1] up from a mere 3.8%[2] five years back. This is by far the best performing solar cell configuration among the other 3rd generation emerging solar cells technologies and is closing onto the performance values of Si-based solar cells. Inspired by the remarkable performance of organic-inorganic perovskite, there have been substantial efforts devoted to understanding the fundamental properties of these materials. Examples of their unique properties include: its large absorption coefficient $\sim 10^4$ cm^{-1}, which is one order of magnitude larger than the N719 dye;[3] its long carrier diffusion length at least 100 nm in $CH_3NH_3PbI_3$[4] and can be as long as ~ 1 μm in $CH_3NH_3PbI_{3-x}Cl_x$,[5] which is a few orders larger than typical solution-processed materials; and its low exciton binding energy (50 meV or less).[6,7] All these properties rationalize the excellent performance of perovskite based solar cells.

Despite the inroads made in understanding the fundamental properties of perovskite solar cells, the interfacial energetics of organic-inorganic perovskite with other functional layers are still not well-studied.[8] Currently, most works simply assume flat band conditions with neither band bending nor interfacial states or interfacial dipoles when considering the band alignments of perovskite with other functional layers.[9–11] However, such simple vacuum level alignment and flat band assumption may not hold true for real interfaces and could lead to misguided interpretation. For example,

[a]Authors to whom correspondence should be addressed. Electronic addresses: Alfred@ntu.edu.sg and Tzechien@ntu.edu.sg

the presence of band bending at the interface would either be beneficial or detrimental to charge transport and affect the resulting device performance; while the presence of interfacial states resulting from interfacial chemical bonding may function as traps for charge carriers and become a loss channel;[12] and the presence of interfacial dipoles would alter the relative positions of the occupied and unoccupied states, and function as electron or hole transfer barriers. Hence, it is of paramount importance that we gain a clear understanding of the interfacial electronic band structure. Recently, a study of 2,2′,7,7′-tetrakis-(*N*,*N*′-di-*p*-methoxyphenyl-amine)-9,9′-spirobifluorene (Spiro-OMeTAD) perovskite interface revealed the absence of interfacial dipoles but the existence of a downward band bending of 0.3 eV in the Spiro-OMeTAD layer[13] that potentially would impede the hole extraction at the interface. With increasing maturity of the perovskite solar cell field, further improvements to the device performances is expected to be increasingly challenging. Therefore, careful interfacial engineering to improve the charge transfer efficiency may hold the key to unleashing the full potential of perovskite solar cells.

In this work, we examine the electronic structure and energy level alignment at the $CH_3NH_3PbI_3$/copper phthalocyanine (CuPc) interface using X-ray photoelectron spectroscopy (XPS) and ultraviolet photoelectron spectroscopy (UPS). Apart from the solution process approach, perovskites can also be prepared by the vapor deposition method, with high efficiency (15%[14]). This opens up the possibility of utilizing an all-evaporated approach similar to that employed small molecule organic solar cells. Here we propose to use CuPc molecules which serve as a prototypical evaporated semiconductor to assess the suitability of CuPc molecules from the energetics point of view. The phthalocyanine family of molecules allow for a wide range of energy level modifications for solar cell applications. CuPc attracts our attention because of its outstanding electronic properties and stability. Furthermore, this molecule has been extensively investigated for a broad range of applications in organic solar cells,[15] organic light emitting diodes,[16] and even organic field effect transistors.[17,18] Our XPS measurements reveal a 0.3 eV downward band bending (away from the interface) in CuPc at 36 nm as validated by UPS measurements. Furthermore, the absence of interfacial dipoles at the CuPc/$CH_3NH_3PbI_3$ interface verifies the validity of utilizing the vacuum level alignment approach for analysis at this interface. In addition, the challenges in preparing such organic-inorganic perovskites for ultra-high vacuum (UHV) studies are also highlighted.

The perovskite samples are prepared by the typical sequential deposition of PbI_2 and CH_3NH_3I into mesoporous TiO_2 substrate.[19] The details of perovskite preparation can be found in Ref. 20. Following which, extreme care was taken when transferring the $CH_3NH_3PbI_3$ sample from the glove box to the XPS analysis chamber to ensure no ambient contact with the sample. To obtain reliable data in this surface sensitive study, it is extremely important to maintain the $CH_3NH_3PbI_3$ surface as pristine as it is prepared, because exposure to the ambient environment will result in decomposition of $CH_3NH_3PbI_3$ to PbI_2 and can affect the XPS analysis. Unlike typical inorganic semiconductor or metal surfaces, the organic groups in perovskite would not allow any form of UHV cleaning. Heating or sputtering of the perovskite under UHV will transform the $CH_3NH_3PbI_3$ surface into PbI_2.[21] To this end, a homemade portable vacuum compatible transfer chamber (complete with gate valve) was used to seal the sample directly in the glove box under N_2 environment. It was then connected to the load-lock of the XPS analysis chambers for transfer, while under a vacuum better than 4×10^{-4} torr. Despite all these measures, our $CH_3NH_3PbI_3$ sample surface inevitably still has a small amount of contaminants like oxygen and carbon from the preparation and glove box. Nonetheless, these measures taken would ensure that the perovskite surface truly reflects a more realistic situation in a practical device.

XPS and UPS measurements are performed on the samples in a home-built UHV multi-chamber system with base pressure better than 1×10^{-9} torr. The XPS source is monochromatic Al K_α with photon energy at 1486.7 eV. The UPS source is from a helium discharge lamp ($h\nu = 21.2$ eV). The photoelectrons are measured by an electron analyzer (Omicron EA125). The CuPc molecules are from Sigma-Aldrich with purity >99% (sublimation grade). The evaporation of CuPc is done in the growth chamber at the pressure better than 5×10^{-9} torr. A Knudsen cell is used to maintain a slow and repeatable growth rate around 2–5 Å/min monitored by a quartz crystal microbalance (QCM) before and after each growth step and further calibrated using XPS attenuation.

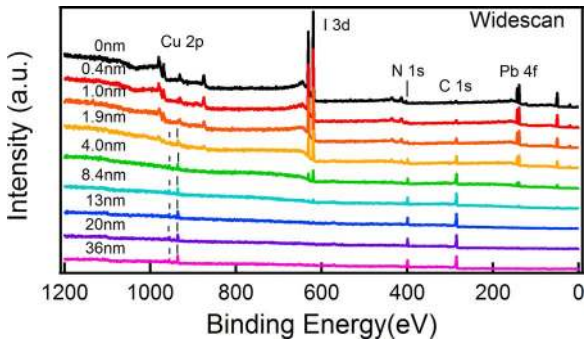

FIG. 1. XPS widescan as a function of CuPc deposition thickness on perovskite.

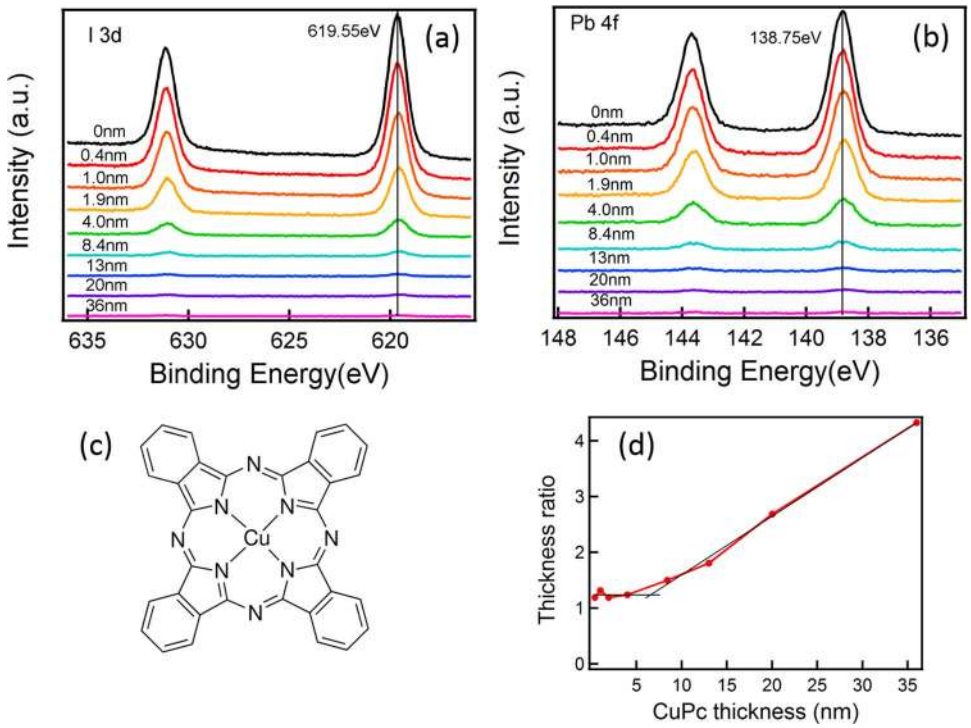

FIG. 2. XPS measurements of perovskite related elements. (a) I 3d; (b) Pb 4f; (c) the molecular structure of CuPc; and (d) thickness ratio between QCM measurement and XPS signal attenuation.

Figure 1 shows the XPS widescans of pristine perovskite and the sequential CuPc deposition. Oxygen presence and adventitious carbon signals in the pristine perovskite are barely observable, indicating our measures taken to avoid air contact have been successful in minimizing surface contamination of the samples. Furthermore, the atomic ratio of nitrogen and lead in surface equals to 0.95 – indicating that the surface organic components of $CH_3NH_3PbI_3$ are still intact and there is minimal PbI_2 formation at the surface. Although $CH_3NH_3PbI_3$ is prepared together with mesoporous TiO_2 as the scaffold, no Ti 2p peak can be found in widescans, confirming that the surface is purely $CH_3NH_3PbI_3$.

Figures 2(a) and 2(b) show the spectra for I 3d and Pb 4f. I 3d5/2 and Pb 4f7/2 peaks are located at 619.55 eV and 138.75 eV, respectively. Both these elements are only present in perovskite, so any potential peak shift will be a good marker of perovskite band bending upon CuPc deposition. We note the absence of any significant broadening of the I 3d and Pb 4f peaks, which rule out any possibility of substrate band bending or interfacial chemical shifts within our detection limits.

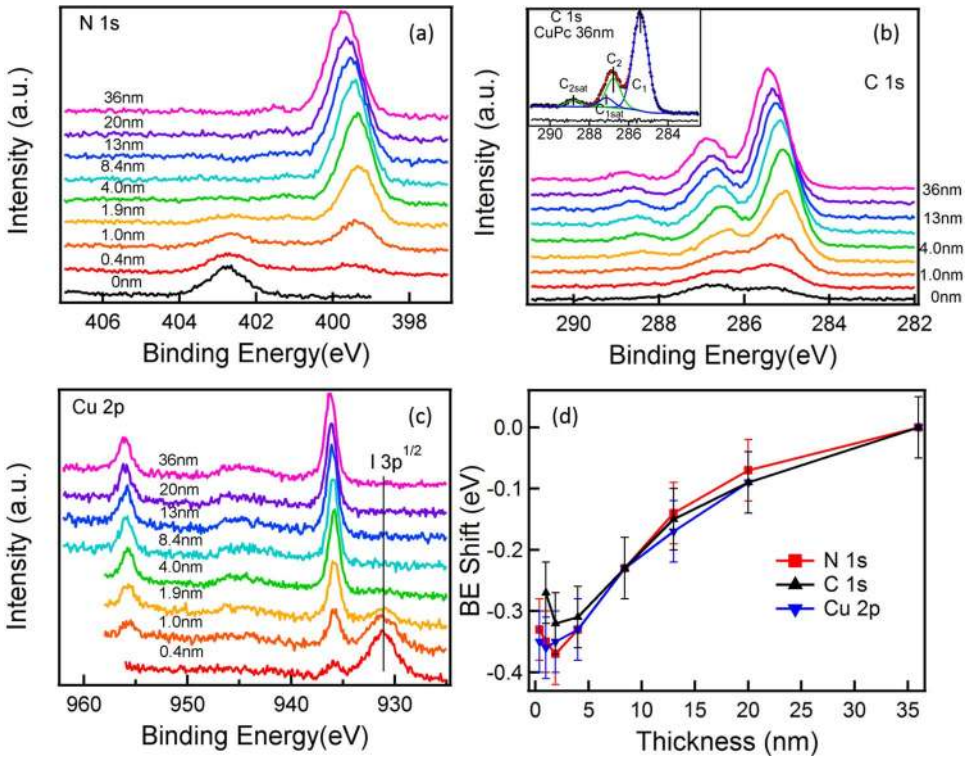

FIG. 3. Narrow scans from N 1s (a), C 1s (b), and Cu2p (c). (d) Binding Energy shift of the three elements in CuPc film. (b) (Inset) Detailed peak fitting of 36 nm CuPc film. C_1, C_{1sat}, C_2, and C_{2sat} represent aromatic carbon, its satellite, pyrrole carbon and its satellite, respectively. The uncertainty of peak position determination is ±0.05 eV.

Careful examination of these two elements suggests no apparent binding energy shift – therefore proving the absence of any band bending of the $CH_3NH_3PbI_3$ after CuPc deposition. The thickness of CuPc film can be estimated from the signal attenuation of the I 3d or Pb 4f peaks. However, when CuPc film thickness increases to beyond a few nanometers, the film thickness estimated by XPS begins to deviate from that measured by the QCM. For instance, both elements are still detectable after 36 nm of CuPc film (as indicated by the QCM). This is obviously incorrect as the electron inelastic mean free path of CuPc layer is only around 2 nm. The thickness ratio (QCM:XPS) between the two methods is shown in Figure 2(d). Up to the first five nanometers, the ratio is close to 1. Beyond 5 nm, the ratio begins to deviate from unity. Such deviation implies that the growth mode of CuPc on perovskite is probably layer-by-layer at the beginning but changes to island growth after a certain critical thickness. This growth phenomenon resembles the Stranski-Krastanov growth mode.

The core level shift of the elements found in CuPc is quite different from that of $CH_3NH_3PbI_3$. The CuPc related elemental spectra (N 1s, C 1s, and Cu 2p) are shown in Figure 3. Although N 1s and C 1s are also present in pristine perovskite surface, the binding energy of these peaks are different from those in CuPc. In N 1s spectra, the peak from $CH_3NH_3PbI_3$ is at 402.7 eV and the peak from CuPc is at 399.7 eV. In C 1s spectra, the peaks at 285.3 eV and 286.8 eV in pristine $CH_3NH_3PbI_3$ are attributed to adventitious carbon and carbon in the methylammonium group of $CH_3NH_3PbI_3$, while the peaks at 285.7 eV, 286.8 eV, and 288.8 eV in 36 nm CuPc film are attributed to aromatic carbon, pyrrole carbon, and its satellite from CuPc, respectively. There is an additional satellite peak at 287.1 eV from aromatic carbon which largely overlaps with pyrrole carbon. The fitting for all four components of C 1s from CuPc is shown in Figure 3(d) inset and our results are in good agreement with previous reports.[22–24] The area ratio of $[C_1+C_{1sat}]/[C_2+C_{2sat}]$ which equates to 3.06, which is close to the ideal the atomic ratio of 3 for aromatic carbon to pyrrole carbon.[22] By monitoring the shifts of the strongest components of N 1s (399.5 eV), C 1s (285.4 eV), and Cu 2p3/2 (936.2 eV), a clear binding energy shift towards higher binding energy side can be seen. The

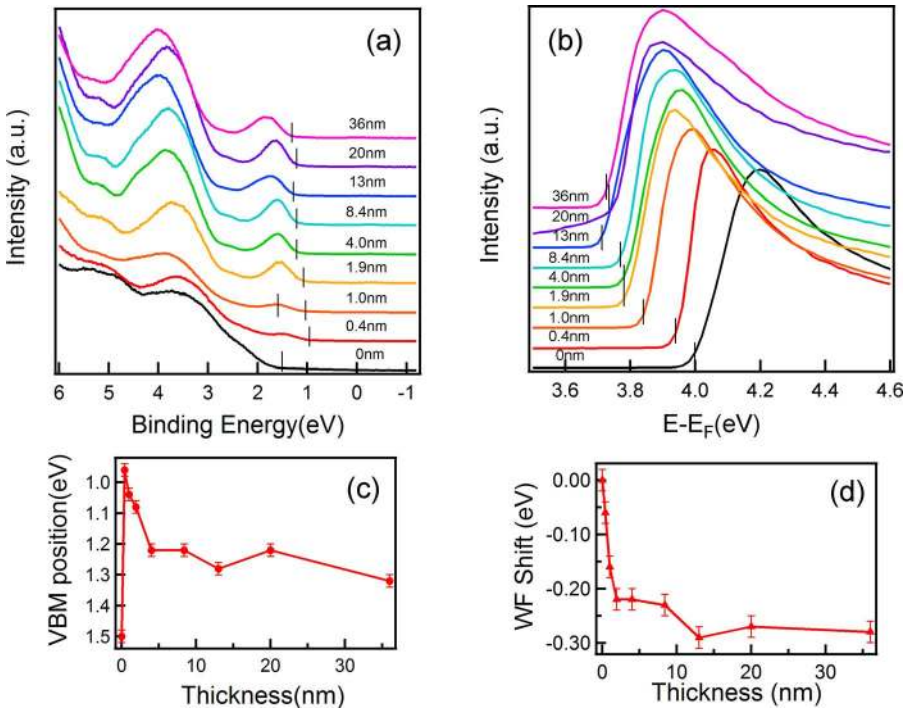

FIG. 4. Valence band (a) and work function (b) from UPS measurements determined from the secondary electron onset; (c) Valance band maximum position; (d) Work function shift. The uncertainty of VBM and WF position determination is ±0.02 eV.

amount of shifts in three elements are shown in Figure 3(d). The binding energy of N 1s and Cu 2p shifts nearly identical towards higher binding energy side up to 0.3 eV, while the C 1s peak shows an additional offset about 0.1 eV. This is due to the coincidental location of the adventitious carbon and the aromatic carbon, causing an additional 0.1 eV shift of the strongest peak in the carbon 1s spectrum. However, this offset will not affect our conclusion because the thicker CuPc film quickly covers the signal from the adventitious carbon and further shift follows exactly the same trend of other elements. Nonetheless, we conclude that there is a 0.3 eV downward band bending in CuPc film.

The thickness-dependent valance band changes and work function shift are measured by UPS. Figure 4 shows the valance band spectra and work function spectra at different CuPc thickness. The valance band maximum (VBM) is determined by linear extrapolation of valance band onset subtracted to the background around Fermi level. As a result, VBM of pristine $CH_3NH_3PbI_3$ is at 1.52 eV below the Fermi level, in good agreement with previous reports.[9,10,25] After CuPc deposition, the HOMO leading edge of CuPc is at 0.96 eV below Fermi level. This onset gradually shifts towards the lower binding energy side up to 1.32 eV – again indicating a band bending in CuPc layer. The work function of the sample also shows a similar shift towards smaller values. The pristine perovskite shows a work function at 4.00 eV, *which is the same as that in a previous report*.[13] After CuPc deposition, the work function gradually shifts to 3.72 eV. The shifts of the VB and work function are summarized at the lower panel of Figure 4. Unlike core level and valance band shifts, the work function shift (less than 0.3 eV) is quickly saturated within 10 nm – likely implying a small reorientation of CuPc molecules at different film thickness.[26–29] However determination of the orientation of the CuPc molecules is beyond the scope of this paper. Therefore, we will only use the core level and the valance band data to discuss the downward band bending trend in the CuPc film.

From these measurements, the complete energy level alignment at $CH_3NH_3PbI_3$/CuPc interface is shown in Figure 5. Before CuPc deposition, the VBM position of pristine perovskite is at 1.52 eV below the Fermi level. Considering the optical bandgap of perovskite is typically around 1.55 eV, the low-lying VBM indicates a strong n-type doping characteristcs. This strong n-type doping of

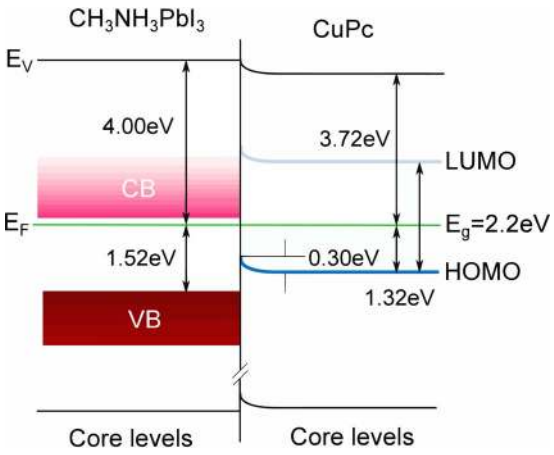

FIG. 5. Energy level diagram of Perovskite/CuPc interface.

the $CH_3NH_3PbI_3$ surface was already observed in other UPS studies.[9,25] At the CuPc side, a 0.3 eV downward bending at 36 nm is observed both from the CuPc XPS and UPS spectra. Due to the lower position of $CH_3NH_3PbI_3$'s VBM as compared to CuPc's HOMO level, hole transfer from perovskite to CuPc is energetically favorable. However, the band bending inside the CuPc film may impede the hole transport away from the interface. Although previous measurements assert the magnitude of downward band bending on Spiro-OMeTAD/$CH_3NH_3PbI_3$ to 0.3 eV, the actual band bending in Spiro-OMeTAD is probably larger as the UPS measurements did not show any abatement at the measured maximum thickness of 8 nm. In contrast, CuPc's band bending at 8 nm is only 0.1–0.2 eV. Therefore, in this respect, CuPc is superior to Spiro-OMeTAD for hole extraction. Obviously, for optimal hole extraction, an upward band bending with suitable energy level alignment is preferred. As demonstrated in a previous paper,[30] the direction of band bending can be tuned by proper doping of materials.

After constructing the energy level alignment diagram, we proceed to estimate the strength of interface dipole at perovskite/CuPc interface using the following equation:[31]

$$pE = \Delta H_{cutoff} - [E_{ion}(CuPc) - E_{ion}(CH_3NH_3PbI_3)], \quad (1)$$

where the ionization energy of E_{ion}(CuPc) and E_{ion}($CH_3NH_3PbI_3$) equals to 5.04 eV and 5.52 eV, repectively, and the VBM energy difference at the interface ΔH_{cutoff} equals to −0.5 eV. The small value of −0.02 eV determined from the above shows that the interface dipole at $CH_3NH_3PbI_3$/CuPc interface can be neglected. We conclude that the CuPc on $CH_3NH_3PbI_3$ shows no strong interfacial dipole formation and can be regarded as vacuum level aligned.

In summary, the energetics at the perovskite/CuPc interface is studied by comprehensive XPS and UPS measurements. XPS measurement reveals a consistent core level shift from CuPc related elemental peaks. UPS further proves this shift in the VB and work function measurements. A 0.3 eV downward band bending in CuPc layer at 36 nm is observed. As the strength of the interface dipole is negligibly small, the interfacial energy alignment is basically via the vacuum level. No strong interfacial dipole formation is observed. Although the hole transfer from perovskite to CuPc is energetically favourable, the band bending may impede the subsequent hole diffusion away from the interface.

We acknowledge the support from the following research grants: NTU start-up Grant Nos. (M4080514, M4080474, and M4081293); SPMS collaborative Research Award (M4080536); the Ministry of Education (MOE) Academic Research Fund (AcRF) Tier 1 Grant No. (M4010808) and Tier 2 Grant No. (M4020176). C.H.A.H. also acknowledges the support of the NTU New Initiative Fund. T.C.S. and N.M. also acknowledge the support from Singapore National Research Foundation through the Singapore-Berkeley Research Initiative for Sustainable Energy (SinBerRISE) CREATE Programme.

[1] R. F. Service, Science **344**, 458 (2014).
[2] A. Kojima, K. Teshima, Y. Shirai, and T. Miyasaka, J. Am. Chem. Soc. **131**(17), 6050 (2009).
[3] S. P. Singh and P. Nagarjuna, Dalton Trans. **43**(14), 5247 (2014).
[4] G. Xing, N. Mathews, S. Sun, S. S. Lim, Y. M. Lam, M. Gratzel, S. Mhaisalkar, and T. C. Sum, Science **342**(6156), 344 (2013).
[5] S. D. Stranks, G. E. Eperon, G. Grancini, C. Menelaou, M. J. P. Alcocer, T. Leijtens, L. M. Herz, A. Petrozza, and H. J. Snaith, Science **342**(6156), 341 (2013).
[6] S. Sun, T. Salim, N. Mathews, M. Duchamp, C. Boothroyd, G. Xing, T. C. Sum, and Y. M. Lam, Energy Environ. Sci. **7**(1), 399 (2014).
[7] V. D'Innocenzo, G. Grancini, M. J. P. Alcocer, A. R. S. Kandada, S. D. Stranks, M. M. Lee, G. Lanzani, H. J. Snaith, and A. Petrozza, Nat. Commun. **5**, 3586 (2014).
[8] J. H. Heo, S. H. Im, J. H. Noh, T. N. Mandal, C. Lim, J. A. Chang, Y. H. Lee, H. Kim, A. Sarkar, Md. K. Nazeeruddin *et al.*, Nat. Photon. **7**(6), 486 (2013).
[9] R. Lindblad, D. Bi, B. Park, J. Oscarsson, M. Gorgoi, H. Siegbahn, M. Odelius, E. M. J. Johansson, and H. Rensmo, J. Phys. Chem. Lett. **5**(4), 648 (2014).
[10] H. Kim, C. Lee, J. Im, K. Lee, T. Moehl, A. Marchioro, S. Moon, R. Humphry-Baker, J. Yum, J. E. Moser, M. Grätzel, and N. Park, Sci. Rep. **2**, 591 (2012).
[11] T. Umebayashi, K. Asai, T. Kondo, and A. Nakao, Phys. Rev. B **67**(15), 155405 (2003).
[12] H. Ishii, K. Sugiyama, E. Ito, and K. Seki, Adv. Mater. **11**(8), 605 (1999).
[13] P. Schulz, E. Edri, S. Kirmayer, G. Hodes, D. Cahen, and A. Kahn, Energy Environ. Sci. **7**(4), 1377 (2014).
[14] M. Liu, M. B. Johnston, and H. J. Snaith, Nature (London) **501**(7467), 395 (2013).
[15] S. Uchida, J. Xue, B. P. Rand, and S. R. Forrest, Appl. Phys. Lett. **84**(21), 4218 (2004).
[16] S. A. Van Slyke, C. H. Chen, and C. W. Tang, Appl. Phys. Lett. **69**(15), 2160 (1996).
[17] J. Wang, H. Wang, X. Yan, H. Huang, and D. Yan, Appl. Phys. Lett. **87**(9), 093507 (2005).
[18] L. Zhen, W. Guan, L. Shang, M. Liu, and G. Liu, J. Phys. D: Appl. Phys. **41**(13), 135111 (2008).
[19] J. Burschka, N. Pellet, S. Moon, R. Humphry-Baker, P. Gao, M. K. Nazeeruddin, and M. Gratzel, Nature (London) **499**(7458), 316 (2013).
[20] S. Dharani, H. K. Mulmudi, N. Yantara, P. T. Thu Trang, N. G. Park, M. Graetzel, S. Mhaisalkar, N. Mathews, and P. P. Boix, Nanoscale **6**(3), 1675 (2014).
[21] T. Supasai, N. Rujisamphan, K. Ullrich, A. Chemseddine, and Th. Dittrich, Appl. Phys. Lett. **103**(18), 183906 (2013).
[22] H. Peisert, M. Knupfer, and J. Fink, Surf. Sci. **515**(2), 491 (2002).
[23] T. Schwieger, H. Peisert, M. Golden, M. Knupfer, and J. Fink, Phys. Rev. B **66**(15), 155207 (2002).
[24] G. Dufour, C. Poncey, F. Rochet, H. Roulet, M. Sacchi, M. De Santis, and M. De Crescenzi, Surf. Sci. **319**(3), 251 (1994).
[25] B. Conings, L. Baeten, C. De Dobbelaere, J. D'Haen, J. Manca, and H. Boyen, Adv. Mater. **26**(13), 2041 (2014).
[26] M. Gorgoi and D. R. T. Zahn, Org. Electron. **6**(4), 168 (2005).
[27] W. Chen, S. Chen, S. Chen, Y. Li Huang, H. Huang, D. Chen Qi, X. Y. Gao, J. Ma, and A. T. S. Wee, J. Appl. Phys. **106**(6), 064910 (2009).
[28] W. Chen, D. Ch. Qi, Y. L. Huang, H. Huang, Y. Z. Wang, S. Chen, X. Y. Gao, and A. T. S. Wee, J. Phys. Chem. C **113**(29), 12832 (2009).
[29] D. Qi, J. Sun, X. Y. Gao, L. Wang, S. Chen, K. P. Loh, and A. T. S. Wee, Langmuir **26**(1), 165 (2010).
[30] C. Hein, E. Mankel, T. Mayer, and W. Jaegermann, Phys. Status Solidi A **206**(12), 2757 (2009).
[31] R. Schlaf, B. A. Parkinson, P. A. Lee, K. W. Nebesny, and N. R. Armstrong, J. Phys. Chem. B **103**(15), 2984 (1999).